DOI: 10.17277/amt.2020.04.pp.058-066

The *I–V* Characteristics of M–$Ba_xSr_{1-x}TiO_3$–M Thin Film Structures with Oxygen Vacancies. Part 2

V.V. Buniatyan*, H.R. Dashtoyan, A.A. Davtyan

National Polytechnic University of Armenia (*NPUA*), *105 Teryan Str., 0009, Yerevan, Armenia*

*Corresponding author. Tel. +3 749 131 16 39. *E-mail*: vbuniat@seua.am, vbuniat@yahoo.com

Abstract

In Part 2 of the paper, based on the results and assumptions pointed in Part 1, analytical expressions were derived for Schottky barrier thermal/field assisted and Poole-Frenkel emission currents. The computer modeling theoretical dependencies of the *I–V* characteristics has been compared with the experimental measured results and obtained good agreements.

Keywords

Ferroelectric; trapping center; Schottky barrier; Poole-Frenkel emission; oxygen vacancy.

© V.V. Buniatyan, H.R. Dashtoyan, A.A. Davtyan, 2020

Hole currents due to thermo-ionic emission

The hole current is associated with the thermo-ionic emission of the holes from the contact 2 [2–5]. For small bias, the effective barrier for holes at contact 2 is $(\Phi_{p2}+\varphi_1-V_2)$. The hole current is given by [2–4]:

$$J_{p2}=A_p^*T^2\exp\left(-\beta(\Phi_{p2}+\varphi_1)\right)(\exp(\beta V_2)-1), \quad (1)$$

for the $V \geq V_{RT}$:

$$\varphi_1-V_2=\frac{\left\{h-\frac{\chi E_{m1}}{qN_A^-}\right\}(|V-V_{FB}|)}{2h}; \quad E_{m1}=\frac{(V+V_{FB})}{h};$$

$$\varphi_1-V_2=\frac{\left\{h-\frac{E_{m1}b}{2}\right\}(|V-V_{FB}|)}{2h};$$

$$\varphi_1-V_2=\frac{\left\{2h-b\frac{(V+V_{FB})}{h}\right\}(V-V_{FB})}{4h}=\left\{\frac{\left[2h^2-b(V+V_{FB})\right](V-V_{FB})}{4h^2}\right\};$$

$$J_{p1}=A_p^*T^2\exp\left(-\beta\Phi_{p2}\right)\times\{\exp(-\beta\varphi_1)\exp(\beta V_2)-\exp(-\beta\varphi_1)\}=A_p^*T^2\exp\left(-\beta\Phi_{p2}\right)\times\{\exp(-\beta(\varphi_1-V_2))-\exp(-\beta\varphi_1)\}.$$

In the neutral region, before the reach–through condition takes place, $V \ll V_{RT}$, the steady-state continuity equation for holes is given by [4]:

$$\frac{\partial^2 P}{\partial x^2}-\frac{P-P_c}{D_p\tau_p}=0, \quad (2)$$

where P_c is the equilibrium hole density, D_p is the diffusion coefficient, and τ_p the lifetime. The solution to (2) is:

$$P-P_c=A\exp\left(\frac{x}{L_p}\right)+B\exp\left(-\frac{x}{L_p}\right), \quad (3)$$

where L_P is the diffusion constant of the holes $\left(L_P=\sqrt{D_P\tau_P}\right)$. The boundary conditions are: $x=d_{f_1}, P\cong P_C\exp\left(-\frac{(\varphi_{f_1}+V_1)}{kT}\right)$, and at $x=d_{f2}$ one has $J_{p_2}^*=A_p^*\exp\left(-\beta(\Phi_{p_2}+\varphi_1-V_2)\right)$, where d_{f1} and d_{f2} are the depletion regions width in the core before the reach–through condition.

The hole current density J_{p1} is then given by the gradient at d_{f1} and the thermal equilibrium condition ($V = 0$) [2–4]:

$$J_{p1} = qD_p \left.\frac{dp}{dx}\right|_{d_{f1}} = \frac{qD_p P_0 \tanh[(d_{f_2} - d_{f_1})L_p]}{L_p} \times$$
$$\times (1 - \exp(-\beta V_1)) + \frac{A_p^* T^2 \exp(-\beta(\Phi_{p2} + \varphi_1))}{\cosh\left[\frac{(d_{f2} - d_{f1})}{L_p}\right]} \times$$
$$\times (\exp(\beta V_2) - 1), \qquad (4)$$

$$J_{p1} = A_p^* T^2 \exp(-\beta \Phi_{F2}) \times$$
$$\times \left\{ \exp\left(-\beta \left[\frac{(V - V_{FB})}{2} - \frac{b(V^2 - V_{FB}^2)}{4h^2} \right] \right) - \exp(-\beta\varphi_1) \right\}. \qquad (5)$$

At $V = V_{FB}$, the factor in $\{\cdot\}$ bracket approaches unity and hole current density is given by:

$$J_{p1} = A_p^* T^2 \exp(-\beta \Phi_{p2}). \qquad (6)$$

For the large voltages, when $V > V_{FB}$, the barrier lowering effect at contact 2 has to be considered due to the applied field and defect caused field (as it was done for the contact 1), and the hole current is now expressed as

$$J_{p1} = A_p^* T^2 \exp(-\beta \Phi_{p2}) \exp(\beta \Delta\Phi_{p2}), \qquad (7)$$

where

$$\Delta\varphi_{p2} = \sqrt{\frac{q(E_{m2} - E_i)}{4\pi\chi_\delta}}.$$

Total current due to thermo-ionic emission

The total current density is found by adding up the contributions of electron current and hole currents. Here the following definitions are used:

Electron saturation current density $J_{ns} = A_n^* T^2 \exp\left(-\frac{q\Phi_{n_1}}{kT}\right)$, hole saturation current density $J_{ps} = A_p^* T^2 \exp\left(-\frac{q\Phi_{p_2}}{kT}\right)$, flat-band voltage $V_{FB} \equiv \frac{L^2}{\xi^2}\gamma$, reach-through voltage $V_{RT} \equiv V_{FB} - 2h\delta_2\gamma$.

For small voltage $V < V_{RT}$, from [1, see (Eq. (7)]:

$$J_{n_1} = A_n^* T^2 \exp(-\beta \Phi_{n_1}) \times$$
$$\times \exp(\beta(\Delta\Phi_{n_1} + \alpha_1 E_{m_1}))(1 - \exp(-\beta V_1)),$$

and from (11) [1]:

$$J = J_{ns} \exp(\beta\Delta\Phi_{n_1})(1 - \exp(-\beta V_1)) +$$
$$+ \frac{qD_p P_o \tanh\left[\frac{(d_{f_2} - d_{f_1})}{L_p}\right]}{L_p}(1 - \exp(-\beta V_1)) +$$
$$+ \frac{J_{ps} \exp(-\beta\varphi_1)}{\cosh\left[\left(\frac{d_{f_2} - d_{f_1}}{L_p}\right)\right]}(\exp(\beta V_2) - 1).$$

For $V_{RT} < V < V_{FB}$ from [1, Eq. (7)] and (2):

$$J = J_{ns} \exp(\beta\Delta\Phi_{n_1}) +$$
$$+ J_{ps} \left\{ \exp\left(-\beta \left[\frac{(V - V_{FB})}{2} - \frac{b(V^2 - V_{FB}^2)}{4L^2} \right] \right) - \exp(-\beta\varphi_1) \right\}.$$

For very large DC bias voltages, $V > V_{FB}$, from Eq. (7) and Eq. (5) [1],

$$J = J_{ns} \exp(\beta\Delta\Phi_{n_1}) + J_{ps} \exp(\beta\Delta\Phi_{p_2}). \qquad (8)$$

Two cases have to be considered:

1) $J_{ns} << J_{ps}$ electron barrier height Φ_{n1} is much larger than the hole barrier height Φ_{p2}. In this case, for the small voltages ($V < V_{rt}$), the hole current is smaller than the electron current. However, for voltages larger than V_{rt} ($V > V_{rt} < V_{FB}$), the hole current dominates;

2) for the $J_{ns} >> J_{ps}$ case, the hole current will be always be smaller than electron current. So that the total current essentially is given by the first term in (8).

Poole–Frenkel mechanism

If the ferroelectric film contains traps for electron and holes, at high temperature and in the presence of an applied high field some of these trapped electrons (holes) will be excited into shallow traps or conduction levels, either thermally or due to the action of the field [1–5, 6–14]. In case the applied field in thin film is up to 1 MV/cm, the Poole–Frenkel emission becomes dominant for the charge separation both in the surface layers [14] and in the core (middle part) of the ferroelectric film. Thus, traps for electrons are assumed to be neutral when occupied and positive charged when empty (i.e., they are donors). Traps for holes are assumed to be neutral when emptied of an electron. For trap states with Coulomb potential, the charge transport is governed by the Poole–Frenkel emission

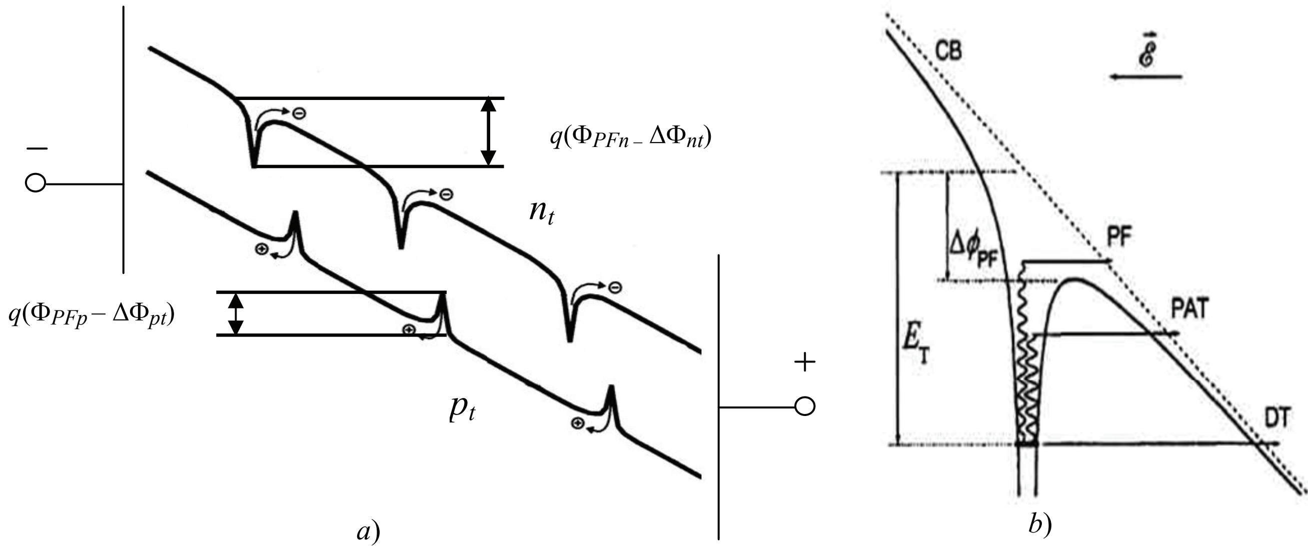

Fig. 1. Lowering of the barriers by $\Delta\Phi_n$ for electrons and $\Delta\Phi_p$ for holes under the applied high field [14] (*a*), energy diagram of the trapping center in the presence of the electric field (*b*) [15–17]

which is very similar to the Schottky emission [2–4, 13, 14]. Fig. 1 helps to analyze the relationship between trapped electrons and holes due to Poole–Frenkel effect [14, 15–17]. Arrows indicate the possible mechanisms of electron emission: thermal ionization over the lowered barrier (PF effect), direct tunneling (DT) into the conduction band (CB), and phonon assisted tunneling (PAT) [15–17].

We assume that ferroelectric film contains traps for electron and for holes, which have E_{tn} and E_{tp} energy levels below the conductance and above the valence bands, respectively. The electron and hole trap densities are denoted by N_{tn} and N_{tp} respectively, Fig. 2. It is assumed that the density of the donor like impurities, particularly the oxygen vacancies, is smaller than that of acceptor like impurities, $N_{tp} > N_{tn}$, i.e. the core (middle part) of the ferroelectric film has poor *p*-type conductivity.

Therefore, if there is no injection of free charge carriers from the contacts and no applied field, it is reasonable to assume, that the for concentration of the holes in the core of ferroelectric will is $(p_{to} - n_{to})$,

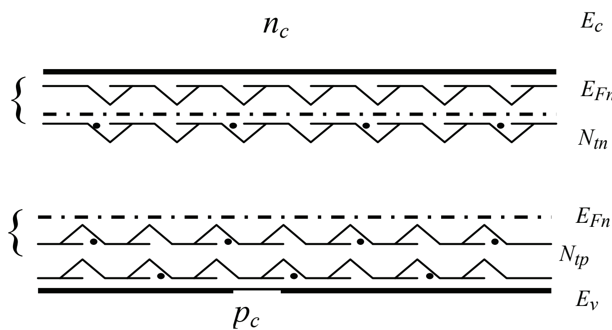

Fig. 2. Trap levels for electron and holes

where n_{to} and p_{to} are the equilibrium concentrations of the trapped electrons and holes. Let the trap densities are given be [15, 18]:

$$N_{tn} = A_{tn}\exp\left(-\frac{E_{tn}}{b_1 kT}\right); \quad N_{tp} = A_{tp}\exp\left(-\frac{E_{tp}}{b_1 kT}\right),$$

where the constants A_{tn}, A_{tp} and b_1 define the shape of the distribution of traps in energy. Using the Shockley–Read–Hall formulation, one may write:

$$\frac{\partial n_t}{\partial t} = r_{1n} - r_{2n}, \quad \frac{\partial P_t}{\partial t} = r_{1p} - r_{2p},$$

where r_{2n}, r_{2p} are the rates of electron and hole release from traps, respectively; r_{1n}, r_{1p} are the rates of electron capture to the conductance band and hole to valence band:

$$r_{1n} = S_n V_{tn} n_c N_{tn}(1 - f_n); \quad r_{1p} = S_p V_{tp} p_c N_{tp}(1 - f_p),$$

here S_n, S_p, V_{tn}, V_{tp} are the capture cross sections and the thermal velocity for the electrons and holes, respectively, n_c and p_c are the free electron and hole concentration in conductance and valence bands, f_n and f_p are the occupancy factor (distribution function) for the electrons and holes respectively. The rates r_{2n}, r_{2p} depends upon the concentration of centers occupied by electrons and holes, and on electron and hole relaxation times τ_{xn} and τ_{xp}; τ_{xn} and τ_{xp} are given by [15, 18]:

$$\tau_{nx} = \left(\frac{1}{\nu_n}\right)\exp\left(\frac{E_{tn}}{kT}\right); \quad \tau_{px} = \left(\frac{1}{\nu_p}\right)\exp\left(\frac{E_{tp}}{kT}\right),$$

where ν_n, ν_p are the "attempt to escape" frequencies for the electrons and holes respectively. Hence, for the r_{2n} and r_{2p} one has:

$$r_{2n} = N_{tn}\, f_n \nu_n \exp\left(-\frac{E_{tn}}{kT}\right);$$

$$r_{2p} = N_{tp}\, f_p\, \nu_p \exp\left(-\frac{E_{tp}}{kT}\right).$$

At the thermal equilibrium $\frac{\partial n_t}{\partial t} = 0, \quad \frac{\partial p_t}{\partial t} = 0,$ and from $r_{1n} = r_{2n}$, $r_{1p} = r_{2p}$ one obtains the concentrations of free electrons and holes:

$$n_c = \frac{f_n \nu_n \exp\left(-\frac{E_{tn}}{kT}\right)}{S_n V_{tn}(1 - f_n)}; \quad p_c = \frac{f_p \nu_p \exp\left(-\frac{E_{tp}}{kT}\right)}{S_p V_{tp}\left(1 - f_p\right)}.$$

In the equilibrium,

$$\left. f_n \right)_{eq} = \left[1 + g_n \exp\left(-\frac{E_{tn}}{kT}\right)\right]^{-1};$$

$$\left. f_p \right)_{eq} = \left[1 + g_p \exp\left(-\frac{E_{tp}}{kT}\right)\right]^{-1},$$

where $g_n = \frac{\nu_n}{S_n V_{tn}}$, $g_p = \frac{\nu_p}{S_p V_{tp}}$.

To use the same detailed balance principle, one can obtain the concentrations of the trapped electrons n_{to} and holes p_{to} in thermal equilibrium:

$$n_{to} = \frac{N_{tn}}{1 + g_n \exp\left(-\frac{E_{tn}}{kT}\right)} = \frac{n_c N_{tn}}{n_c + n_1};$$

$$p_{to} = \frac{N_{tp}}{1 + g_p \exp\left(-\frac{E_{tp}}{kT}\right)} = \frac{p_c N_{tp}}{p_c + p_1},$$

where n_1 and p_1 are the Shockley–Read state factors for the electron and hole respectively (i.e., the concentration of electrons and holes in conductance and valence bands, when the quasi-Fermi levels coincides with the trap levels). Consequently, in equilibrium the concentrations of ionized donors and ionized acceptors are:

$$n_d^+ = n_d - n_{to}; \quad n_a^- = n_a - p_{to},$$

n_d and n_a are respectively the concentrations of the donors and acceptors.

Now the Poole–Frenkel emission will be considered assuming the contact *1* [1, see Fig. 3] being reverse biased and contact 2 forward biased. For $V > V_{Fn}$ the current density is given by:

$$J = J_{ns} \exp\left(\beta_s \Delta\Phi_{n1}\right) + J_{ps} \exp\left(\beta_s \Delta\Phi_{p2}\right),$$

where $\beta_s = \left(\frac{q}{kT}\right)\left(\frac{q}{\pi\chi_f}\right)^{1/2};$

$$J = J_{ns} \exp\left(\beta_s (E_{m2})^{1/2}\right) + J_{ps} \exp\left(\beta_s (E_{m2})^{1/2}\right);$$

$$J = J_o \exp\left(\beta_s (E_m(0))^{1/2}\right). \quad (9)$$

When the Poole–Frenkel emission becomes dominant, the continuity of steady-state current inside the film requires that J is constant and independent of the position in the film. Thus, neglecting diffusion, since the electric field is high, J may be given by

$$J = qn_c(x)\mu_n E(x) + qp_c(x)\mu_p E(x), \quad (10)$$

where $n_c(x)$, $p_c(x)$, μ_n, μ_p are correspondingly the free electron and hole concentrations due to Poole–Frenkel emission and mobilities.

Under the Poole–Frenkel emission the electric field distribution in the ferroelectric may be determined from the Poisson's equation:

$$\frac{dE}{dx} = -\frac{q}{\chi_f}\left\{N_{tp}\left(1 - F_p(x)\right) - N_{tn}\left(1 - F_n(x)\right) + p_c + n_c\right\}, \quad (11)$$

where $F_n(x)$ and $F_p(x)$ are the coordinate dependent trap occupations of the electrons and holes in the film; p_c and n_c are respectively the free hole and electron concentrations.

Let $n_{tn}(x)$ be the filled trap density of electrons and $p_{tp}(x)$ be the filled trap density of holes at position x. Then the Poisson's equation may be written as (direction of electric field is the negative x axis):

$$\frac{dE}{dx} = -\frac{q}{\chi_f}\left[P_{tp}(x) - n_{tn}(x) + p_c - n_c\right]. \quad (12)$$

Let the electron capture rate from conduction band be r_{1n} and electron release rate from traps be r_{2n} and from the holes r_{1p} and r_{2p}, respectively. Considering an infinitesimal trap energy range between E_t and $E_t + dE_t$ the expressions for r_{1n}, r_{1p} can be written, respectively, as:

$$r_{1n} = n_c N_{tn}\left(1 - f_n(x)\right) S_n V_{tn} dE_t;$$

$$r_{1p} = p_c N_{tp}\left(1 - f_p(x)\right) S_p V_{tp} dE_t,$$

where $f_n(x)$ and $f_p(x)$ are occupancy factors for the electron and holes, respectively. They depend on the trap energy and position in the film [15, 18]:

$$F_n(x)=\frac{\int_0^h f_n(x)N_{tn}dE_t|}{\int_0^h N_{tn}dE_t};\quad F_p(x)=\frac{\int_0^h f_p(x)N_{tp}dE_t|}{\int_0^h N_{tp}dE_t}.$$

The electron and hole release rates r_{2n}, r_{2p} depend on the concentrations of centers which are occupied by electrons and holes and on the electron and hole relaxation times τ_n, τ_p [15, 18]:

$$\tau_n=\left(\frac{1}{\nu_n}\right)\exp\left[\frac{(E_{tn}-\Delta\Phi_{tn})}{kT}\right];$$

$$\tau_p=\left(\frac{1}{\nu_p}\right)\exp\left[\frac{(E_{tp}-\Delta\Phi_{tp})}{kT}\right].$$

where ν_n, ν_p are the attempt to escape frequencies, while $\Delta\Phi_{tn}$, $\Delta\Phi_{pt}$ represent the lowering of the tarp barrier heights assuming the Poole–Frenkel mechanism, i.e.,

$$\Delta\Phi_{tn}=\beta_{PF}kTE^{1/2};\quad \Delta\Phi_{tp}=\beta_{PF}kTE^{1/2},$$

where β_{PF} is the slope of the $\log J\sim E^{1/2}$ plot when the Poole–Frenkel mechanism dominates the condition:

$$\beta_{PF}=2\beta_s,\quad \beta_s=\left(\frac{q}{kT}\right)\left(\frac{q}{\pi\chi_f}\right)^{1/2}.$$

The barrier lowering in the case of the Poole–Frenkel emission differs by a factor 2 from the one for the Schottky emission due to the immobility of the ionic centers emitting the charges [2–4]. Therefore, for the r_{2n} and r_{2p} take the form:

$$r_{2n}=N_{tn}f_n\nu_n\exp\left(-\frac{E_{tn}}{kT}\right)\exp\left(\beta_{PF}E^{1/2}\right)dE_t;$$

$$r_{2p}=N_{tp}f_p\nu_p\exp\left(-\frac{E_{tp}}{kT}\right)\exp\left(\beta_{PF}E^{1/2}\right)dE_t,$$

assuming, that the trap densities are given by:

$$N_{tn}=kT\ A_{tn}\exp\left(-\frac{E_{tn}}{b_1kT}\right);$$

$$N_{tp}=kT\ A_{tp}\exp\left(-\frac{E_{tp}}{b_1kT}\right).$$

As it was noted:

$$J=J_{ns}\exp\left[\beta_sE_{m1}(0)^{1/2}\right]+J_{ps}\exp\left[\beta_sE_{m1}(0)^{1/2}\right].\quad(13)$$

Equating r_{1n} to r_{2n}, and r_{1p} to r_{2p} and using (10) and (13), for the occupancy factors f_n and f_p one arrives at:

$$f_n=\left\{1+\left(\frac{\nu_n\mu_nq}{J_{ns}S_nV_{tn}}\right)E(x)\exp\left[\beta_{PF}(E(x))^{1/2}\right]\times\times\exp\left[-\beta_s(E(0))^{1/2}\right]\exp\left(-\frac{E_{tn}}{kT}\right)\right\}^{-1};$$

$$f_p=\left\{1+\left(\frac{\nu_p\mu_pq}{J_{ps}S_pV_{tp}}\right)E(x)\exp\left[\beta_{PF}(E(x))^{1/2}\right]\times\times\exp\left[-\beta_s(E(0))^{1/2}\right]\exp\left(-\frac{E_{tp}}{kT}\right)\right\}^{-1}.\quad(14)$$

Then the density of the trapped electrons and holes $n_{tn}(x)$ and $p_{tn}(x)$ are:

$$n_{tn}(x)=\int_0^{E_{tn}}f_nN_{tn}dE_t;\quad p_{tp}(x)=\int_0^{E_{tp}}f_pN_{tp}dE_t.$$

Assuming $E_{tn}>b_1kT$, $E_{tp}>b_1kT$ one may rewrite f_n and f_p as:

$$f_n=\frac{1}{1+\gamma_o\gamma_n\exp\left(-\frac{E_{tn}}{kT}\right)};$$

$$f_p=\frac{1}{1+\gamma_o\gamma_p\exp\left(-\frac{E_{tp}}{kT}\right)},$$

with

$$\gamma_n=\left(\frac{\nu_n\mu_nq}{J_{ns}S_nV_{tn}}\right)\exp\left[-\beta_sE_{m1}^{1/2}\right],$$

$$\gamma_p=\left(\frac{\nu_p\mu_pq}{J_{ps}S_pV_{tp}}\right)\exp\left[-\beta_sE_{m1}^{1/2}\right].$$

For the $n_{tn}(x)$ and $p_{tp}(x)$ one has:

$$n_{tn}(x)=\int_0^{E_{tn}}\frac{A_{tn}dE_t\exp\left(-\frac{E_{tn}}{bkT}\right)}{\left[1+\gamma_0\gamma_n\exp\left(-\frac{E_{tn}}{kT}\right)\right]},\ \text{or}$$

$$n_{tn}(x) \cong \frac{A_{tn} b_1 kT}{\gamma_0 \gamma_n (b_1 - 1)} \exp\left[\frac{E_{tn}(b_1 - 1)}{kTb_1}\right];$$

$$p_{tp}(x) = \int_0^{E_{tp}} \frac{A_{tp} dE_t \exp\left(-\frac{E_{tp}}{bkT}\right)}{\left[1 + \gamma_0 \gamma_p \exp\left(-\frac{E_{tp}}{kT}\right)\right]}, \text{ or}$$

$$p_{tn}(x) \cong \frac{A_{tp} b_1 kT}{\gamma_0 \gamma_n (b_1 - 1)} \exp\left[\frac{E_{tp}(b_1 - 1)}{kTb_1}\right];$$

$$\gamma_0 = E(x) \exp\left[\beta_{PF} (E(x))^{1/2}\right].$$

Now the Poisson's equation may be solved and the voltage drop across the film calculated:

$$V = \int_0^h E(x) dx .$$

As it is evident from (11) and (12), $E(x)$ depends on the concentrations of captured and free charge carriers, which, in turn, depend on $E(x)$ via γ_n, γ_p exponentially. Hence the Poisson's equation is impossible to solve analytically. In this paper, for numerical simulations, an average value of electric field is used:

$$E_{fav}(x) = \frac{V_f}{h - 2\delta_1},$$

where $V_f = \left| V - \frac{(V^2 + V_{FB}{}^2)}{2V_{FB}} \right|$ is the voltage drop in the core of the ferroelectric film.

If the concentration of the donor (vacancies) is n_d, the concentration of ionized donors is $n_d^+ = n_d - n_{tn}$, and at the same time $n_d^+ = n_c$ (that is concentration of free electrons), then $n_c = n_d - n_{tn}$,

$$n_c = n_d - n_{tn} = n_d - \frac{A_{tn} b_1 kT J_{ns} S_n V_{tn} \exp\left(\beta_s (E_{m1})^{1/2}\right)}{\gamma_0 \nu_n \mu_n q (b_1 - 1)} \times$$
$$\times \exp\left[\frac{E_{tn}(b_1 - 1)}{b_1 kT}\right],$$

and

$$J_{ns} = \frac{(n_d - n_c)\gamma_0 \nu_n \mu_n q (b_1 - 1)}{A_{tn} b_1 kT S_n V_{tn} \exp\left(\beta_s (E_{m1})^{1/2}\right) \exp\left[\frac{E_{tn}(b - 1)}{b_1 kT}\right]}.$$

Similarly, for the J_{ps}:

$$J_{ps} = \frac{(n_a - p_c)\gamma_0 \nu_p \mu_n q (b_1 - 1)}{A_{tp} b_1 kT S_p V_{tp} \exp\left(\beta_s (E_{m2})^{1/2}\right) \exp\left[\frac{E_{tp}(b_1 - 1)}{b_1 kT}\right]}.$$

Substituting for the J_{ns} and J_{ps} in (13) on arrives at:

$$J = \frac{\gamma_0 \nu_n \mu_n q (n_d - n_c)(b_1 - 1)}{A_{tn} b_1 kT S_n V_{tn}} \exp\left[-\frac{(b_1 - 1)E_{tp}}{b_1 kT}\right] +$$
$$+ \frac{\gamma_0 \nu_p \mu_p q (n_a - p_c)(b_1 - 1)}{A_{tp} b_1 kT S_p V_{tp}} \exp\left[-\frac{(b_1 - 1)E_{tp}}{b_1 kT}\right]. \quad (15)$$

Assuming $S_n = S_p$, $A_{tn} = A_{tp} = A_o$, $\nu_n = \nu_p = \nu_o$, $E_{tn} = E_{tp} = E_t$, one can obtain

$$J = \sigma_{PF} E(x) \exp\left\{\beta_{PF} [E(x)]^{1/2}\right\}, \quad (16)$$

where

$$\sigma_{PF} = \frac{q\nu_o (b_1 - 1)}{b_1 kT A_o S_o} \left[\frac{\mu_n (n_d - n_c)}{V_{tn}} + \frac{\mu_p (n_a - p_c)}{V_{tp}}\right] \times$$
$$\times \exp\left[-\frac{(b_1 - 1)E_t}{b_1 kT}\right]. \quad (17)$$

Note, that the expression (15) is distinctive for the Poole-Frenkel emission [2–4, 8–10, 13–22].

Experimental

The test capacitors are fabricated on high resistivity (> 5 kOhm·cm) silicon substrate [21]. The commercially available template used has $Pt/TiO_2/SiO_2/Si(100)$ structure. Pt (50 nm) / Au (500 nm) bottom electrode is deposited by e-beam evaporation at room temperature (Fig. 3). The 560 nm thick $Ba_{0.25}Sr_{0.75}TiO_3$ (BSTO) film is deposited by pulsed laser ablation from a stoichiometric $Ba_{0.25}Sr_{0.75}TiO_3$ target at 650 °C and 0.4 mBar oxygen pressure using a KrF examiner laser ($\lambda = 248$ nm, $\tau = 30$ ns) operating at 10 Hz with an energy density of 1.5 Jcm^2. After deposition, the sample is cooled down to room temperature at 950 mBar oxygen pressure. The Au (500 nm) / Pt (50 nm) top electrode are deposited by e-beam evaporation at room temperature and patterned with a lift-off process. The *I–V* performance is measured using HP415B semiconductor parameter analyzer (Fig. 4) [21].

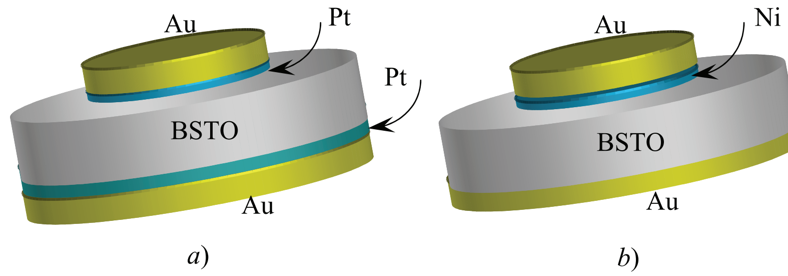

Fig. 3. Structures of the test varactor with Au (a) and Pt (b) interfaces

Calculations and discussions

In this section the expressions of (1) – (17) are used to investigate the dependence of the *I–V* on various parameters, and more specifically on the parameters of the oxygen vacancies associated traps. Symmetrical structures [1, see Fig. 2], with contact *1* forward biased and contact *2* reverse biased are considered. The results of the numerical simulations using (8) are denoted as S_{ch} and correspond to the Schottky barrier emission. The results of the simulations using (15) are denoted as PF and correspond to the Poole–Frenkel emission. The numerical calculations have been carried out for the following values of the parameters: cross section area $S_o \sim (6-8)\cdot 10^{-6}$ cm^2, thickness of the film: $h = 550$ nm, 30 μm diameter [21, 22], the electron and hole mobilities are: $\mu_{no} \cong 10^{-2}$ cm/Vs and $\mu_{po} \cong$ $\cong 10^{-2}$ cm/Vs respectively [6–8, 13, 23], the barrier heights: $\phi_{n1} \approx 0.9$ V, $\phi_{p2} \approx 0.5$ V [8, 9, 15, 24], $T = 300$ K, the dielectric constant of the interface region with high density of oxygen vacancies: $\chi_\delta \approx 1.5-5$, the dielectric constant of the ferroelectric film core: $\chi_f \approx 290$ [6, 15, 21–23], $\xi_o \approx 10^{-1}-10^{-2}$, $E_{tn} = 0.1-0.4$ eV, $E_{tp} = 0.2-1$ eV, $b_1 = 10$, $m_p^*/m_0 = 10$, $m_n^*/m_0 = 10$, the conductivity of core: $\sigma_0 \approx 10^{-12}$ sm, the concentration of free electrons and holes, respectively $n_c \approx 10^{14}-10^{17}$ cm^{-3}, $n_p \approx 10^{14}-10^{17}$ cm^{-3}, the concentration of the trapped electrons and holes $n_t \approx 10^3-10^6$ cm^{-3}, $p_t \approx 10^3-10^6$ cm^{-3}, the thermal velocity of carriers $v_{tp} \approx 10^7$ cm/s, the capture cross sections $S_n = S_p = 10^{-16}$ cm^2, the attempt to escape frequencies $\upsilon = 10^{12}$ s^{-1}.

The results of the numerical simulations are shown in Fig. 4 where the experimental results for comparison are also presented.

The Richardson's constants have been calculated by:

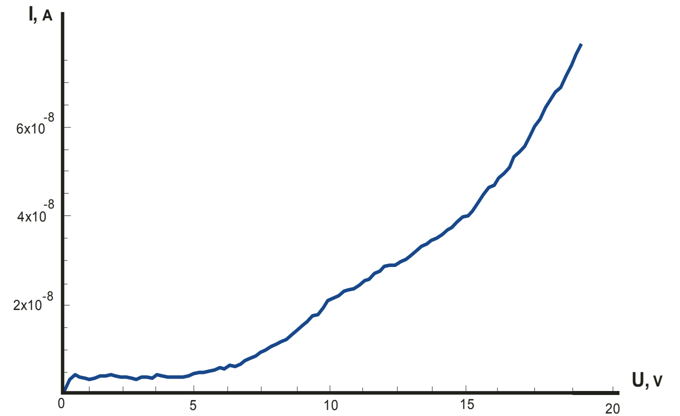

Fig. 4. Experimental *I–V* dependence of a Pt/Ba$_{0.25}$Sr$_{0.75}$TiO$_3$/Pt parallel-plate ferroelectric capacitor
($S_o \sim 7\cdot 10^{-6}$ cm^2, sample: T21, 550 nm thick BST, 30 μm diameter, $\chi_f \approx 290$ [21, 22])

$$A^*_n \approx \frac{4\pi q m_n^* k^2}{h_p{}^3}; \quad A^*_p \approx \frac{4\pi q m_p^* k^2}{h_p{}^3},$$

where h_p is the Plank's constant.

For the thermo-ionic field (Schottky) emission:

$$I_{ns} = \frac{A^*_n T^2}{\exp(\beta\Delta\Phi_{n1})}; \quad I_{ps} = \frac{A^*_p T^2}{\exp(\beta\Delta\Phi_{n2})};$$

$$I_{st} = 4.9\cdot 10^{-8} T^2 S_0 \left(m_{n0}^* \exp\left(4.64\left(\frac{V+V_{FB}}{\chi_{\delta 0} h_0}\right)^{1/2}\right) + \right.$$

$$\left. + m_{p0}^* \exp\left(4.64\left(\frac{V-V_{FB}}{\chi_{\delta 0} h_0}\right)^{1/2}\right)\right).$$

For the Poole–Frenkel emission:

$$I_{PF} = S_0 \gamma_0 \sigma_0; \quad \gamma_0 = E(x)\exp\left(\beta E^{1/2}(x)\right),$$

$$E_{fav}(x) = \frac{V_f}{h - 2\delta_1},$$

$$V_f = \left| V - \frac{\left(V^2 + V_{FB}{}^2\right)}{2V_{FB}} \right|$$ is the voltage drop in ferroelectric core,

$$\sigma_0 = \frac{q\nu(b_1 - 1)}{b_1 kTA_{tn}} \left[\frac{\mu_n(n_j - n_c)}{S_n V_{tn}} \exp\left(-\frac{(b_1 - 1)E_{tn}}{KT} \right) + \right.$$
$$\left. + \frac{\mu_p(n_a - n_c)}{S_p V_{tp}} \exp\left(-\frac{(b_1 - 1)E_{tp}}{kT} \right) \right],$$

$$I_{PF} = 12 \cdot 10^{-3} S_0 \frac{|V_f|}{h} \left(\mu_{n0} n_t + \mu_{p0} p_t \right) \times$$
$$\times \exp\left(0.06 \left(\frac{|V_f|}{h\,\chi_{f0}} \right)^{1/2} \right).$$

The total current is taken as a sum of $I = I_{St} + I_{PF}$.

As it is evident from Fig. 5, there is a fairly good agreement between the experimental curves and theoretical calculations. For the bias voltages up to 12–13 V the *I–V* dependence may be explained by Schottky emission in punch-through (flat-band) regime. With the applied voltage increased, the Poole–Frenkel emissions from the trap levels begin to start and when $V > (12–13)$ V, the leakage current is associated simultaneously by the Schottky barrier and the Poole–Frenkel emission. The small discrepancy between the theory and experiments may be explained, first of all, by the difference between the symmetric model used in the analysis, asymmetric Pt/BST/Pt structure used in the experiment. Furthermore, the electric field in the core of ferroelectric film was approximated by $E_{fav} = V_f / (h - 2\delta_1)$. For accurate calculations one has to take into account the *x*-coordinate dependence of the electric field according to the Poisson's equation. And finally, the mobility is not known exactly.

It is also necessary to note, that our analysis is based on the hydrogen model of impurities in crystalline dielectrics, i.e. in approximation of the Coulombic potential, which is valid for relatively shallow levels. The precise shape of potential wells corresponding to deep levels may different from the Coulombic form. The second point is follow: while in Schottky mechanism the lowering of the barrier occurs uniformly for all direction of carrier motion in the hemisphere centered on the direction of the field, i.e. the probability of escape is enhanced by the same factor $\exp\left(\beta_s E^{1/2} / kT\right)$ for all attempted directions of escape,

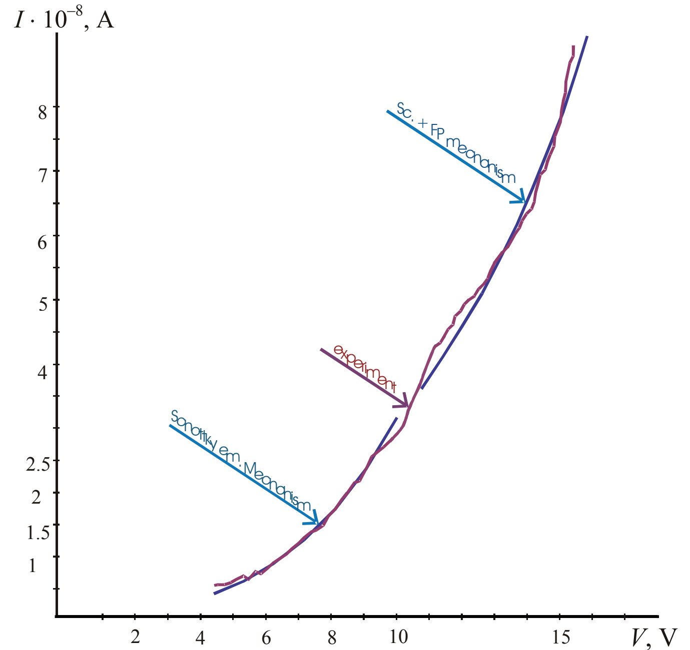

Fig. 5. Theoretical and experimental *I–V* characteristics of Pt/BST/Pt structure
(sample: T21: 550 nm thick, $Ba_{0.25}Sr_{0.75}TiO_3$, 30 μm diameter, $\chi_f = 290$ [21], $x_\delta = 5$, the other parameters are chosen as: $\xi_0 = n_c / n_p = 0.8$, $\varphi_k \approx 0.7$ eV, $E_{tn} = 0.2$ eV, $E_{tp} = 0.36$ eV, $V_{th} = 10^7$ cm/s, $\mu_n = 0.01$ cm²/Vs, $\mu_p = 0.005$ cm²/Vs, $\upsilon = 10^{12}$ s^{-1}, $n_c = 1.5 \cdot 10^{15}$ cm^{-3}, $n_p = 1.0 \cdot 10^{14}$ cm^{-3}, $n_t = 10^6$ cm^{-3}, $p_t = 10^6$ cm^{-3}, $S_n = S_p = 10^{-16}$ cm², $b_1 = 10$)

the situation for the Poole–Frenkel effect is more complicate. In this case it is necessary to take into account the effect of the angle between the direction of escape and the direction of the field *E*. The received expression (14) based the model, on which the maximum barrier lowering $\left\{\beta_{PF}[E(x)]^{1/2}\right\}$ occurs only in one particular direction in space, all other directions having to overcome a higher barrier. The measured *I–V* and the theoretical estimations of the emission process unambiguously indicate that the Poole–Frenkel emission is compatible with the Schottky field emission mechanism. The Poole–Frenkel emission takes place in the range of higher voltages. The analysis of the PF effect indicates that the active trapping centers are located in the region of very high electric field exceeding 10^5 V/cm. The field of such strength is concentrated at the middle part of ferroelectric film. The space charge is assumed to be related to deep trapping centers and oxygen vacancies. In the discussed applied voltage polarity case [1, see Fig. 2) the carrier injected mainly are holes [1, see Fig. 2, from

contacts 2]. According to the energy band diagram of the Pt/BST/Pt films, the hole injection is much more favorable than the electron injection.

From the practical point of view, the further understanding of the mechanism of the trapping/detrapping process may allow to characterize hysteresis effects and the noise in devices based on Pt/BST/Pt structures. And finally, the proposed theory may be useful for the analysis of similar structures based on other perovskite ferroelectrics.

Acknowledgments

The study was supported by RA MESCS Science Committee as part of the research project No. 19YR–2J050.

The authors would like to thank Prof. S. Gevorgian and Dr. Andrei Vorobiev from Department of Microtechnology and Nanoscience (Chalmers University of Technology, Gothenburg, Sweden), for stimulating discussions and providing experimental results.

References

1. Buniatyan V.V., Dashtoyan H.R. The *I–V* Characteristics of M–$Ba_xSr_{1-x}TiO_3$–M Thin Film Structures with Oxygen Vacancies. Part 1, *Advanced Materials & Technologies*, 2020, *1*(17), 8-17.

2. Tagantsev A.K., Sherman V.O., Astafiev K.F. et al. Ferroelectric Materials for Microwave Tunable applications. *J. of Electroceramics*, 2003, *11*, 5-66.

3. Sze S.M. Current Transport and Maximum Dielectric Strength of Silicon Nitride Films. *J. Appl. Phys.*, 1967, *38*, 2951-2956.

4. Sze S., Coleman D., Loya A. Current transport in Metal-Semiconductor-Metal (MSM) structures. *Solid State Electronics*, 1971, *14*, 1209-1218.

5. Sze S.M., Kwok K.Ng. *Physics of Semiconductor Devices*. A John Wiley & Sons, Inc., Publ., 2007, 816 p.

6. Tagantsev A.K. and Gerra G. Interface-induced phenomena in polarization response of ferroelectric thin films. *J. Appl. Phys.,*2006, *100*, 052607-1-28.

6. O'Dwer J.J. Current–Voltage Characteristics of Dielectric Films. *J. Appl. Phys.*, 1966, *37*(2), 599-601.

7. Scott J.F., Aranjo C.A., Melnick B.M., et al. Quantitative measurement of space–charge effects in lead ziconate-titanate memories. *J. Appl. Phys.*, 1991, *70*(70), 382-388.

8. Dietz G.W., Antpohler W., Klee M., et al. Electrode influence on the charge transport through $SrTiO_3$ thin films. *J. Appl. Phys*., 1995, *78*, 6113-6118.

9. Saha S., Kaufman D.X., Streiffer S.K., et al. Anomalous leakage current characteris tics of Pt/($Ba_{0.75}$,$Sr_{0.25}$)$Ti_{1+y}O_{3+z}$/Pt) thin films grown by metal – organic chemical vapor deposition. *J. Appl. Phys.,* 2003, *28*(24), 3866-3868.

10. Zafar S., Jones R. E., Jiang Bo, et al. The electronic conduction mechanism in barium strontium titanate thin films. *J. Appl. Phys. Lett*., 1998, *73*(24), 3533-3535.

11. Stolichnov I. and Tagantsev A. Space–Charge influenced-injection model for conduction in $Pb(Zr_xTi_{1-x})O_3$ thin films. *J. Appl. Phys.*, 1998, *84*(6), 3216-3225.

12. Gevorgian S.Sh. *Ferroelectrics in Microwave Devices*, *Circuits and Systems*. Springer-Verlag, London, 2009, 394 p.

13. Dawber M., Raba J.F., Scott J.F. Physics of thin-film ferroelectric oxides. *Rev. of Modern Phys.*, 2005, *77*, 1083-1130.

14. Grossmann M., Lohse O., Bolten D., et al. The interface screening model as origin of imrint in $PbZr_xTi_{1-x}O_3$ thin films. Numerical simulation and verification. *J. Appl. Phys.*, 2002, *92*(5), 2688-2696.

15. Ongaro R., Pillonnet A. Poole-Frenkel (PF) effect high field saturation. *Revue de Physique Appliquee*, 1989, *24*, 1085-1095.

16. Mitrofanov O., Manfra M.J. Poole–Frenkel electron emission from the traps in AlGaN/GaN transistors. *J. Appl. Phys.*, 2004, *95*, 6414-6419.

17. Antula J. Hot-electron concept for Poole–Frenkel conduction in amorphous dielectric solids. *J. Appl. Phys.*, 1972, *94*(11), 4663-4668.

18. Pulfrey D.L., Shousha A.H.M. and Young L. Electronic Conduction and Space Charge in Amorphous Insulating Films. *J. Appl. Phys.*, 1970, *41*(7), 2838-2834.

19. Baniecki J.D., Laibonitz R. B., Shaw T.M., et al. Hidrogen induced tunnel emission in Pt/(Ba_xSr_{1-x})$Ti_{1+y}O_{3+z}$/Pt thin films Capacitors. *J. Appl. Phys*., 2001, *89*(5), 2873-2885.

20. Simmons J.G. Theory of Metallic Contacts on High resistivity Solids. *J. Phys. Chem. Solids*, 1971, *32*, 2581-2591.

21. Vorobiev A., Rundgvist P., Gevorgian S., Microwave loss mechanisms in $Ba_{0.25}Si_{0.75}TiO_3$ films. *J. Appl. Phys.*, 2004, *96*, 4642-4649.

22. Gevorgian S.Sh. *Ferroelectrics in Microwave Devices, Circuits and Systems*. Springer-Verlag, London, 2009, 394 p.

23. Newille R.C., Hoencisen B. Anomalous capacitance of Schottky barriers on strontium titanate. *J. Appl. Phys*., 1975, *46*(1), 350-353.